Machine Intelligence & Robotic Control, Vol. 5, No. 3, 87–93 (2003)

Paper

Nonlinear Lateral Control of Vision Driven Autonomous Vehicles*

Miguel Ángel Sotelo†

Abstract: This paper presents the results of a lateral control strategy that has been applied to the problem of steering an autonomous vehicle using vision. The lateral control law has been designed for any kind of car-like vehicle presenting the Ackerman kinematic model, accounting for the vehicle velocity as a crucial parameter for adapting the steering control response. This makes the control strategy suitable for either low or high speed vehicles. The stability of the control law has been analytically proved and experimentally tested by autonomously steering Babieca, a Citroen Berlingo prototype vehicle.

Keywords: Vehicle Control, Chained Systems Theory, Vision Driven Autonomous Vehicles

1. Introduction

LATERAL automatic steering of autonomous car-like vehicles has become an apparent field of application for robotics researchers. Basically, this problem can be stated as that of determining an appropriate control law for commanding the vehicle steering angle. Many steering control designs are already documented in the literature [1], [3], [6]. A comparative study on various lateral control strategies for autonomous vehicles can be found in [11], where a linearized model of the lateral vehicle dynamics is used for controller design based on the fact that it is possible to decouple the longitudinal and lateral dynamics. On the contrary, a simplified nonlinear lateral kinematic model is proposed in this work to ease the design and implementation of a stable lateral control law for autonomous steering of car-like vehicles. The lateral control strategy was implemented on Babieca, an electric Citroen Berlingo experimental prototype, using vision as the main sensor to measure the position of the vehicle on the road. Real tests were carried out on a private circuit, emulating an urban quarter, composed of streets, intersections (crossroads), and roundabouts, located at the Industrial Automation Institute (IAI) in Arganda del Rey, Madrid. Additionally, a live demonstration exhibiting the system capacities on autonomous steering was carried out during the IEEE Conference on Intelligent Vehicles 2002, in a private circuit located at Satory (Versailles), France.

2. Lateral Control

Considering the case of an autonomous vehicle driving along some reference trajectory, the main goal of the lateral control module is to ensure proper tracking of the reference trajectory by correctly keeping the vehicle in the center of the lane with the appropriate orientation (parallel to the desired trajectory). This constraint can be generalized as the minimization of the lateral and orientation errors of the vehicle (d_e, θ_e) with respect to the reference trajectory, at a control point, as illustrated in **Fig. 1**. To solve this controllability problem and design a stable lateral controller, a model describing the dynamic behavior of d_e and θ_e is needed.

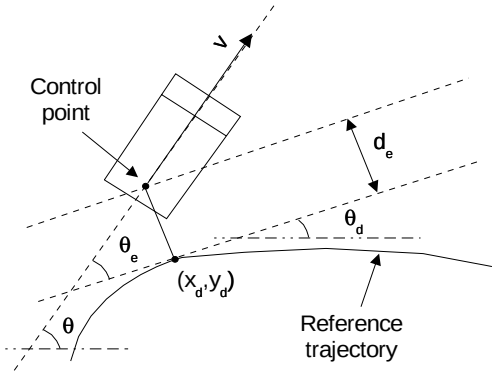

Fig. 1 Lateral and orientation errors at the look-ahead distance

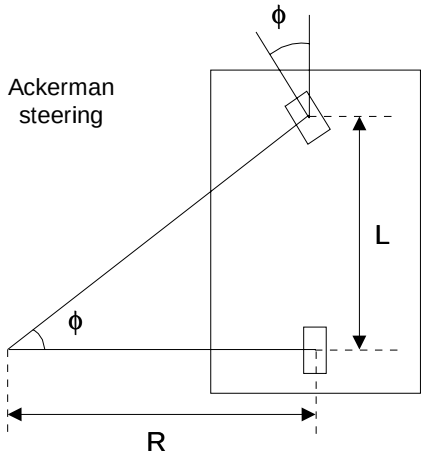

Fig. 2 Approximate kinematic model of the vehicle (Ackerman steering)

2.1 Kinematic model

The kinematic model of the vehicle is the starting point to model the dynamics of the lateral and orientation errors. The vehicle model is approximated by the popular Ackerman (or bicycle) model [4] as depicted in **Fig. 2**, assum-

* Received 20 August, 2003; accepted 13 October, 2003.

† Department of Electronics. Technical School, University of Alcalá, Campus Universitario s/n, 28871 Alcalá de Henares, Madrid, Spain. E-mail: michael@depeca.uah.es

ing that the two front wheels turn slightly differentially and thus, the instantaneous rotation center can be purely computed by kinematic means. Let $\kappa(t)$ denote the instantaneous curvature of the trajectory described by the vehicle:

$$\kappa(t) = \frac{1}{R(t)} = \frac{\tan\phi(t)}{L} = \frac{d\theta(t)}{ds} \tag{1}$$

where R is the radius of curvature, L is the wheelbase, ϕ is the steering angle, and θ stands for the vehicle orientation in a global frame of coordinates. The dynamics of θ is computed in Eq. (2) as a function of vehicle velocity v:

$$\dot{\theta} = \frac{d\theta}{dt} = \frac{d\theta}{ds}\frac{ds}{dt} = \kappa(t)v(t) = \frac{\tan\phi(t)}{L}v(t). \tag{2}$$

Let ϕ and v be the variables of the vehicle control input space. On the other hand, the vehicle configuration space is composed of the global position and orientation variables, described by (x, y, θ), under the flat terrain assumption. Mapping from the control input space to the configuration space can be solved by using the popular Fresnel equations, which are also the so-called dead reckoning equations typically used in inertial navigation. Equation (3) shows the dynamics of (x, y, θ):

$$\begin{aligned} \dot{x} &= \frac{dx}{dt} = v(t)\cos\theta(t) \\ \dot{y} &= \frac{dy}{dt} = v(t)\sin\theta(t) \\ \dot{\theta} &= \frac{d\theta}{dt} = v(t)\frac{\tan\phi(t)}{L} \end{aligned} \tag{3}$$

where $v(t)$ represents the velocity of the midpoint of the rear axle of the vehicle, denoted as the control point. Global information about the position and orientation of the vehicle (x, y, θ) is then transformed so as to develop a model that describes the open-loop lateral and orientation error dynamics. As observed in Fig. 1, the lateral error d_e is defined as the distance between the vehicle control point and the closest point along the vehicle desired trajectory, described by coordinates (x_d, y_d). This implies that d_e is perpendicular to the tangent to the reference trajectory at (x_d, y_d). The scope of the tangent at (x_d, y_d) is denoted by θ_d and represents the desired orientation at that point. Based on this, d_e and θ_e suffice to precisely characterize the location error between the vehicle and some given reference trajectory, as described in Eqs. (4) and (5):

$$d_e = -(x - x_d)\sin\theta_d + (y - y_d)\cos\theta_d \tag{4}$$

$$\theta_e = \theta - \theta_d. \tag{5}$$

Computing the derivative of d_e with respect to time yields Eq. (6), while the time derivative of θ_e is shown in Eq. (7):

$$\begin{aligned} \dot{d}_e &= -\dot{x}\sin\theta_d + \dot{y}\cos\theta_d \\ &= -V\cos\theta\sin\theta_d + V\sin\theta\cos\theta_d \\ &= V\sin(\theta - \theta_d) \\ &= V\sin\theta_e \end{aligned} \tag{6}$$

$$\dot{\theta}_e = \frac{d(\theta - \theta_d)}{dt} = \dot{\theta} - \dot{\theta}_d = \dot{\theta}. \tag{7}$$

Thus, the complete nonlinear model for d_e and θ_e is formulated in Eq. (8):

$$\begin{aligned} \dot{d}_e &= V\sin\theta_e \\ \dot{\theta}_e &= \tfrac{V}{L}\tan\phi. \end{aligned} \tag{8}$$

2.2 Nonlinear control law

The control objective is to ensure that the vehicle will correctly track the reference trajectory. For this purpose, both the lateral error d_e and the orientation error θ_e must be minimized. On the other hand, for simplicity, vehicle velocity v will be assumed to be constant. The design of the control law is based on general results of the so-called chained systems theory. An excellent example on this topic can be found in [5]. Nevertheless, these results are extended and generalized in this paper so as to provide a stable nonlinear control law for steering of Ackerman-like vehicles, based on local errors. From the control point of view, the use of the popular tangent linearization approach is avoided as it is only valid locally around the configuration chosen to perform the linearization, and thus, the initial conditions may be far away from the reference trajectory. On the contrary, some state and control variable changes are posed in order to convert the nonlinear system described in Eq. (8) into a linear one, without any approximation (exact linearization approach). Nevertheless, due to the impossibility of exactly linearizing the systems describing mobile robots dynamics, these nonlinear systems are converted into almost linear ones, termed as chained forms. The use of the chained form permits to design a control law using linear systems theory to a higher extent. In particular, the nonlinear model for d_e and θ_e (Eq. (8)) can be transformed into chained form using the state diffeomorphism and the change of control variables as in Eq. (9):

$$\begin{aligned} Y = \begin{bmatrix} y_1 \\ y_2 \end{bmatrix} = \Theta(X) = \begin{bmatrix} d_e \\ \tan\theta_e \end{bmatrix} \\ W = \begin{bmatrix} w_1 \\ w_2 \end{bmatrix} = \Upsilon(U) = \begin{bmatrix} v\cos\theta_e \\ \dfrac{v\tan\phi}{L\cos^2\theta_e} \end{bmatrix}. \end{aligned} \tag{9}$$

These transformations are invertible whenever the vehicle speed v is different from zero and the orientation error θ_e is different from $\pi/2$. This implies that the singularities of the transformations can be avoided by assuring that the vehicle moves ($v > 0$) and that its orientation error is maintained under 90 degrees (the vehicle orientation must not be perpendicular to the reference trajectory). These conditions are reasonably simple to meet in practice. From Eq. (9), the vehicle model can be rewritten as in Eq. (10), considering y_1 and y_2 as the new state variables:

$$\begin{aligned} \dot{y}_1 &= \dot{d}_e = v\sin\theta_e = w_1 y_2 \\ \dot{y}_2 &= \frac{d(\tan\theta_e)}{dt} = \frac{1}{\cos^2\theta_e}\dot{\theta}_e = \frac{v\tan\phi}{L\cos^2\theta_e} = w_2. \end{aligned} \tag{10}$$

In order to get a velocity independent control law, the time derivative is replaced by a derivation with respect to ς, the abscissa along the tangent to the reference trajectory

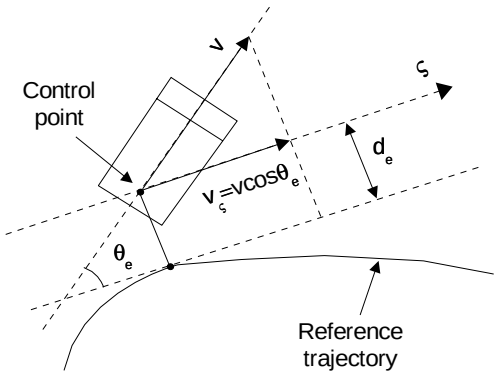

Fig. 3 Graphical description of ς

as graphically depicted in **Fig. 3**. Analytically, ς is computed as the integral of velocity v_ς, measured along axis ς:

$$\begin{aligned} \varsigma &= \int v_\varsigma dt = \int v \cos\theta_e dt \\ \Rightarrow \dot{\varsigma} &= \frac{d\varsigma}{dt} = v\cos\theta_e = w_1. \end{aligned} \tag{11}$$

The time derivatives of the state variables y_1 and y_2 are expressed as functions of ς in Eq. (12):

$$\begin{aligned} \dot{y}_1 &= \frac{dy_1}{dt} = \frac{dy_1}{d\varsigma}\frac{d\varsigma}{dt} = y_1'\dot{\varsigma} \\ \dot{y}_2 &= \frac{dy_2}{dt} = \frac{dy_2}{d\varsigma}\frac{d\varsigma}{dt} = y_2'\dot{\varsigma} \end{aligned} \tag{12}$$

where y_1' and y_2' stand for the derivatives of y_1 and y_2 with respect to ς. Solving for y_1' and y_2' yields Eq. (13):

$$\begin{aligned} y_1' &= \frac{\dot{y}_1}{\dot{\varsigma}} = \frac{v\sin\theta_e}{v\cos\theta_e} = \tan\theta_e = y_2 \\ y_2' &= \frac{\dot{y}_2}{\dot{\varsigma}} = \frac{v\tan\phi}{L\cos^2\theta_e v\cos\theta_e} = \frac{\tan\phi}{L\cos^3\theta_e} = \frac{w_2}{w_1} = w_3. \end{aligned} \tag{13}$$

As observed in the previous equation, the transformed system is linear and thus, state variables y_1 and y_2 can be regulated to zero (so as to yield $d_e = d_{e,ref} = 0$ and $\theta_e = \theta_{e,ref} = 0$) by using the control low proposed in Eq. (14):

$$w_3 = -K_d y_2 - K_p y_1, \quad (K_d, K_p) \in \Re^{+2}. \tag{14}$$

Using Eqs. (13) and (14) and solving for variable y_1 yields Eq. (15):

$$y_1'' + K_d y_1' + K_p y_1 = 0 \tag{15}$$

where the dynamic behavior of y_1 with respect to ς is proved to be linear.

Under the assumption of positive values for constants K_d and K_p, variable y_1 tends to zero as long as variable ς grows. In fact, variable y_1 has a second order linear dynamic behaviour dominated by two poles with negative real components. According to this, y_1 tends to zero as the independent variable (ς in this case, not time) tends to infinite. This statement ensures that d_e tends to zero as ς tends to infinite as dictated by Eq. (9) ($y_1 = d_e$). From Eq. (13), if y_1 is zero, then y_2 is also zero ($y_2 = y_1'$). Likewise, if y_2 is zero then θ_e is zero from Eq. (9) ($y_2 = \tan\theta_e$). Thus, both variables y_1 and y_2 tend to zero as variable ς grows. The previous statement is analytically expressed in Eq. (16):

$$\lim_{\varsigma\to\infty} d_e = \lim_{\varsigma\to\infty} \theta_e = 0. \tag{16}$$

Accordingly, variable ς must always grow so as to ensure that both d_e and θ_e tend to zero. This condition is met whenever $v > 0$ and $-\pi/2 < \theta_e < \pi/2$. In other words, the vehicle must continuously move forward and the absolute value of its orientation error should be below $\pi/2$ in order to guarantee proper trajectory tracking. Thus, the nonlinear control law is finally derived from Eqs. (13) and (14) such that

$$\phi = \arctan\left[-L\cos^3\theta_e(K_d\tan\theta_e + K_p d_e)\right]. \tag{17}$$

The control law is then modified by a sigmoidal function as shown in Eq. (18) to account for the physical limitations in the vehicle wheels turning angle and prevent from actuator saturation:

$$\phi = \arctan\left[-KL\cos^3\theta_e \frac{1-\exp^{-K(K_d\tan\theta_e + K_p d_e)}}{1+\exp^{-K(K_d\tan\theta_e + K_p d_e)}}\right] \tag{18}$$

On the other hand, the use of sigmoidal functions preserves the system stability [10].

The control law is saturated to $\phi_{\max}$ by properly tuning parameter K. Thus, the maximum value of Eq. (18) is $\phi_{\max} = \pm\arctan(-KL)$. Therefore, K is chosen to ensure that $\phi_{\max} = \pm\pi/6$ rad (physical limitation of the vehicle) given the wheelbase $L = 2.69$ m, yielding a practical value $K = 0.2146$:

$$K = \frac{\tan\frac{\pi}{6}}{L}. \tag{19}$$

From observation of Eq. (15), the dynamic response of the variable y_1 can be considered to be a second order linear one. In practice, it is not indeed linear due to the sigmoidal function used to saturate the control law, although it can be reasonably approximated as such. Thus, an analogy between constants K_d, K_p and the parameters of a second order linear system, ξ (damping coefficient) and ω_n (natural frequency), can be established, yielding Eq. (20):

$$\begin{aligned} \omega_n &= \sqrt{K_p} \\ \xi &= \frac{K_d}{2\sqrt{K_p}}. \end{aligned} \tag{20}$$

Likewise, system overshoot M_p and settling distance d_s (given that the system error dynamics is described as a function of space variable ς, not time) can be obtained from Eq. (21):

$$\begin{aligned} M_p &= \exp^{\frac{-\xi\pi}{\sqrt{1-\xi^2}}} \\ d_{s|2\%} &= \frac{4}{\xi\omega_n}. \end{aligned} \tag{21}$$

The design of constants K_d and K_p is undertaken considering that the system overshoot must not exceed 10%

of the step input and the settling distance should be below some given threshold. Thus, for a typical settling time $t_s = 20$ s and given a vehicle velocity v, the proper settling distance can be computed as in Eq. (22):

$$d_s = t_s v = 20v. \tag{22}$$

The value of K_d is derived from Eqs. (20) and (21) yielding the velocity dependant expression in Eq. (23):

$$K_d = \frac{8}{d_s} = \frac{0.4}{v}. \tag{23}$$

Likewise, damping coefficient ξ is derived from Eqs. (20) and (21), as shown in Eq. (24):

$$\xi = \sqrt{\frac{1}{\left(\frac{\pi}{\ln 0.1}\right)^2 + 1}} = \frac{K_d}{2\sqrt{K_p}} = \frac{4}{d_s\sqrt{K_p}}. \tag{24}$$

Finally, K_p is deduced from the previous equation, yielding Eq. (25):

$$K_p = \left(\frac{6.766}{d_s}\right)^2 = \left(\frac{0.3383}{v}\right)^2. \tag{25}$$

The dependency of K_p and K_d on the vehicle velocity v permits to ensure proper dynamic response. In particular, vehicle turning angle will be smooth at high speeds, therefore avoiding possible oscillations due to physical constraints in steering dynamics.

2.3 Extension of the control law for high speeds

The nonlinear control law designed in the previous section provides stable trajectory tracking for Ackerman-like vehicles at moderate speeds (up to 10–20 km/h). This makes the previous control law suitable for low speed vehicles. However, experience demonstrates that tracking errors and vehicle oscillation increase as velocity rises. Then it becomes necessary to develop an extension of the nonlinear control law for high speeds. The first step is to modify the vehicle control point as depicted in **Fig. 4**, in order to anticipate the trajectory curvature at a given distance L_h denoted by Look-ahead distance. The new lateral and orientation errors are then computed as illustrated in the same Fig. 4, yielding the results in Eq. (26):

$$\begin{aligned} d_e &= -(x + L_h\cos\theta - x_d)\sin\theta_d \\ &\quad +(y + L_h\sin\theta_d - y_d)\cos\theta_d \\ \theta_e &= \theta - \theta_d. \end{aligned} \tag{26}$$

The choice of L_h is carried out based on the current vehicle velocity v, as described in [3], yielding the parameters shown in Eq. (27):

$$L_h(v) = \begin{cases} L_{\min} & \text{if } v < v_{\min} \\ vt_1 & \text{if } v_{\min} \le v \le v_{\max} \\ L_{\max} & \text{if } v > v_{\max} \end{cases} \tag{27}$$

where $t_1 = 1.5$ s is the look-ahead time, $v_{\min} = 25$ km/h, $v_{\max} = 75$ km/h, $L_{\min} = 10.41$ m, and $L_{\max} = 31.25$ m. Considering the same scheme followed in the previous section, the new nonlinear model for d_e and θ_e is shown in Eq. (28):

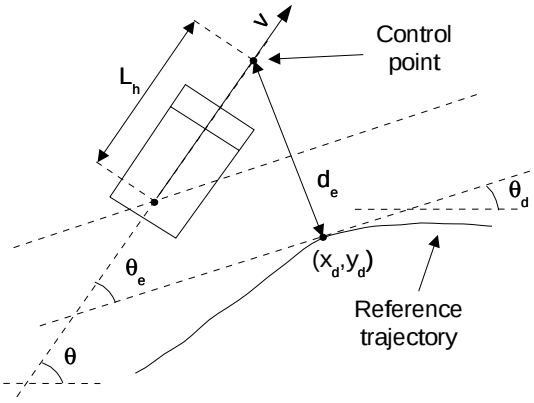

Fig. 4 Lateral and orientation errors at the look-ahead distance

$$\begin{aligned} \dot{d}_e &= v\sin\theta_e + \frac{vL_h}{L}\cos\theta_e\tan\phi \\ \dot{\theta}_e &= \frac{v\tan\phi}{L}. \end{aligned} \tag{28}$$

This model can be transformed into chained form using the state diffeomorphism and change of control variables, as in Eq. (29):

$$Y = \begin{bmatrix} y_1 \\ y_2 \end{bmatrix} = \Theta(X) = \begin{bmatrix} d_e \\ \tan\theta_e \end{bmatrix}$$

$$W = \begin{bmatrix} w_1 \\ w_2 \end{bmatrix} = \Upsilon(U) = \begin{bmatrix} v\cos\theta_e + \dfrac{vL_h\cos^2\theta_e\tan\phi}{L\sin\theta_e} \\ \dfrac{v\tan\phi}{L\cos^2\theta_e} \end{bmatrix}. \tag{29}$$

These transformations are invertible whenever the vehicle speed v is different from zero and the orientation error θ_e is different from $\pi/2$. From Eq. (28) the vehicle dynamic model can be rewritten as in Eq. (30), considering y_1 and y_2 as the new state variables:

$$\begin{aligned} \dot{y}_1 &= \dot{d}_e = v\sin\theta_e + \frac{vL_h}{L}\cos\theta_e\tan\phi = w_1 y_2 \\ \dot{y}_2 &= \frac{d(\tan\theta_e)}{dt} = \frac{1}{\cos^2\theta_e}\dot{\theta}_e = \frac{v\tan\phi}{L\cos^2\theta_e} = w_2. \end{aligned} \tag{30}$$

In order to get a velocity independent control law, the time derivative is replaced by a derivation with respect to ς, a variable related to the abscissa along the tangent to the reference trajectory. Analytically, ς is computed according to the following expression:

$$\varsigma = \int \left(v\cos\theta_e + \frac{vL_h\cos^2\theta_e\tan\phi}{L\sin\theta_e}\right) dt. \tag{31}$$

The time derivatives of the state variables y_1 and y_2 are expressed as functions of ς in Eq. (32):

$$\begin{aligned} \dot{y}_1 &= \frac{dy_1}{dt} = \frac{dy_1}{d\varsigma}\frac{d\varsigma}{dt} = y_1'\dot{\varsigma} \\ \dot{y}_2 &= \frac{dy_2}{dt} = \frac{dy_2}{d\varsigma}\frac{d\varsigma}{dt} = y_2'\dot{\varsigma} \end{aligned} \tag{32}$$

where y_1' and y_2' stand for the derivatives of y_1 and y_2 with respect to ς, respectively. Solving for y_1' and y_2' yields Eq. (33):

$$\begin{aligned} y_1' &= \tan\theta_e = y_2 \\ y_2' &= \frac{\tan\phi}{L\cos^3\theta_e + L_h \dfrac{\cos^4\theta_e \tan\phi}{\sin\theta_e}} = w_3. \end{aligned} \tag{33}$$

As in the previous section, the transformed system is linear and thus, state variables y_1 and y_2 can be regulated to zero (so as to yield $d_e = d_{e,ref} = 0$ and $\theta_e = \theta_{e,ref} = 0$) by using the new control low proposed in Eq. (34):

$$w_3 = -K_d y_2 - K_p y_1 \qquad (K_d, K_p) \in \Re^{+2}. \tag{34}$$

Using Eqs. (33) and (34) and solving for variable y_1 yields Eq. (35):

$$y_1'' + K_d y_1' + K_p y_1 = 0 \tag{35}$$

where the dynamic behaviour of y_1 with respect to ς is proved to be linear.

Once again, this implies that variables $y_1 (= d_e)$ and $y_2 (= \tan\theta_e)$ tend to zero as variable ς grows. The previous statement is analytically expressed in Eq. (36):

$$\lim_{\varsigma\to\infty} d_e = \lim_{\varsigma\to\infty} \theta_e = 0. \tag{36}$$

Accordingly, variable ς must always grow so as to ensure that both d_e and θ_e tend to zero. This condition is met whenever $v > 0$ and $-\pi/2 < \theta_e < \pi/2$. In other words, the vehicle must continuously move forward and the absolute value of its orientation error should be below $\pi/2$ in order to guarantee proper trajectory tracking. Basically, stability conditions remain the same as in the previous section. Thus, the new nonlinear control law for high speeds is finally derived from Eqs. (33) and (34) such that

$$\phi = \arctan\left[\frac{-L\sin\theta_e\cos^3\theta_e(K_d\tan\theta_e + K_p d_e)}{\sin\theta_e + L_h\cos^4\theta_e(K_d\tan\theta_e + K_p d_e)}\right]. \tag{37}$$

The control law is then modified by a sigmoidal function to account for the physical limitations in the vehicle wheels turning angle and prevent from actuator saturation. From this point onwards, tuning of K, K_d, and K_p follows the same scheme derived in Eqs. (19), (23), and (25), respectively.

3. Implementation and Results

The control law for autonomous steering described in this paper was tested on the so-called Babieca prototype vehicle (an electric Citroen Berlingo), as depicted in **Fig. 5**. The vehicle was modified to allow for automatic velocity and steering control at a maximum speed of 90 km/h. Babieca is equipped with a color camera to provide lateral and orientation position of the ego-vehicle with regard to the center of the lane, a Pentium PC, and a set of electronic devices to provide actuation over the accelerator and steering wheel, as well as to encode the vehicle velocity and steering angle. The color camera provides standard PAL video signal at 25 Hz that is processed by a Meteor frame grabber installed on a 120 MHz Pentium running the Real Time Linux operating system. The complete navigation system, implemented under Real Time Linux using a pre-emptive scheduler, runs a vision-based lane tracking task for computing the lateral and orientation errors.

Fig. 5 Babieca prototype vehicle

Practical experiments were conducted on a private circuit located at the Industrial Automation Institute in Arganda del Rey (Madrid). The circuit is composed of several streets, intersections, and roundabout points, trying to emulate an urban quarter. Various practical trials were conducted so as to test the validity of the control law for different initial conditions in real circumstances. During the tests, the reference vehicle velocity is kept constant by a velocity controller. Coefficients K_d and K_p were calculated as a function of v using Eqs. (19) and (21). **Figures 6** and **7** show the transient response of the lateral and orientation errors of the vehicle for reference velocities of 20 km/h and 50 km/h respectively. In both cases, the vehicle starts the run at an initial lateral error of about 1m and an initial orientation error in the range $\pm 5^\circ$. For illustrative purposes, **Fig. 8** depicts the steering control provided by the controller during the path tracking experiment carried out at 50 km/h. As can be clearly appreciated, the steady state response of the system is satisfactory for either experiments. Thus, the lateral error is bound to ± 5 cm at low speeds and ± 25 cm at $v = 50$ km/h, while the absolute orientation error in steady state remains below 1° in all cases. Just to give an example on how the practical results conform to the expected values as derived from the theoretical development, let's consider the transient response of the vehicle depicted in Fig. 6 for $v = 20$ km/h. Assuming a theoretical maximum overshoot of $M_p = 10\%$ and a settling time of $t_s = 20$ s, the controller coefficients are tuned to $K_d = 0.072$ and $K_p = 0.0037$, according to Eqs. (19) and (21). Nonetheless, from observation of Fig. 6 the maximum overshoot obtained in practice yields up to almost 25% for both the lateral and orientation errors, while the settling time takes some 22 s. This is mainly due to the existence of nonlinear actuator dynamics and latencies, which are not considered in the model. In spite of these slight differences with regard to the theoretical expected values, the practical results exhibited in this section demonstrate that the nonlinear lateral control law developed in this work still permits to safely steer the vehicle at operational velocities.

In a final trial, the results achieved in the second test for

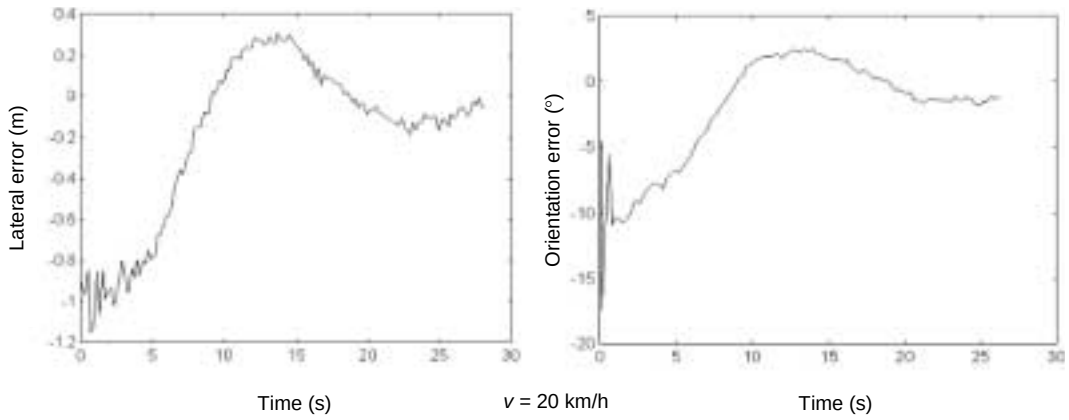

Fig. 6 Transient response of the lateral and orientation error for $v = 20$ km/h

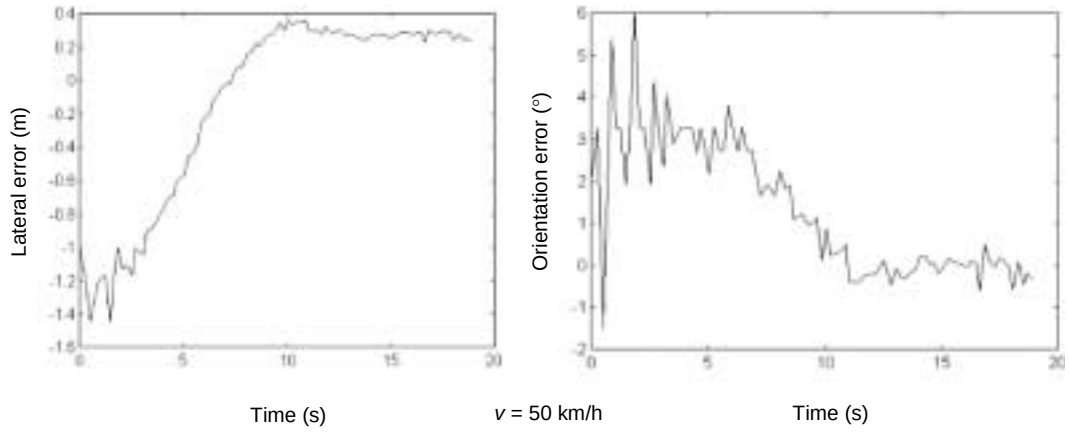

Fig. 7 Transient response of the lateral and orientation error for $v = 50$ km/h

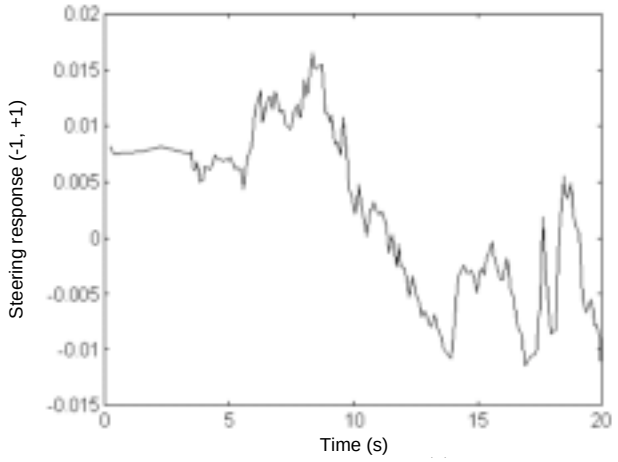

Fig. 8 Steering normalized response (between -1 and $+1$) for $v = 50$ km/h

$v = 20$ km/h are compared to human driving at the same speed along the same trajectory. For this purpose a human driver steered the vehicle, leaving the control of the accelerator to the velocity controller in order to keep a reference speed of 20 km/h. The comparison is graphically depicted in **Fig. 9**.

One can observe that the human driver takes less time than the automatic controller to achieve lateral and orientation errors close to zero. On the other hand, the steady state errors are similar in both cases. Surprisingly, human driving turns out in sporadic separations from the reference trajectory up to 40–50 cm, without incurring in dangerous behavior, while the automatic controller keeps the vehicle under lower lateral error values once stabilized. Far from being an isolated fact, this circumstance was repeatedly observed in several practical experiments. As the conclusion, the lateral control law developed in this work can reasonably be considered to be valid for driving a car-like vehicle as precisely as a human can. During the last year, Babieca ran over hundreds of kilometers in lots of successful autonomous missions carried out along the test circuit using the nonlinear control law described in this paper. A live demonstration exhibiting the system capacities on autonomous driving using the nonlinear control law described in this paper was carried out during the IEEE Conference on Intelligent Vehicles 2002, in a private circuit located at Satory (Versailles), France. A complete set of video files demonstrating the operational performance of the control system in real test circuits (both in Arganda del Rey and in Satory) can be retrieved from ftp://www.depeca.uah.es/pub/vision.

4. Conclusions

To conclude, the next key points should be remarked.

- First of all, the nonlinear control law described in this work has proved its empirical stability for lateral driv-

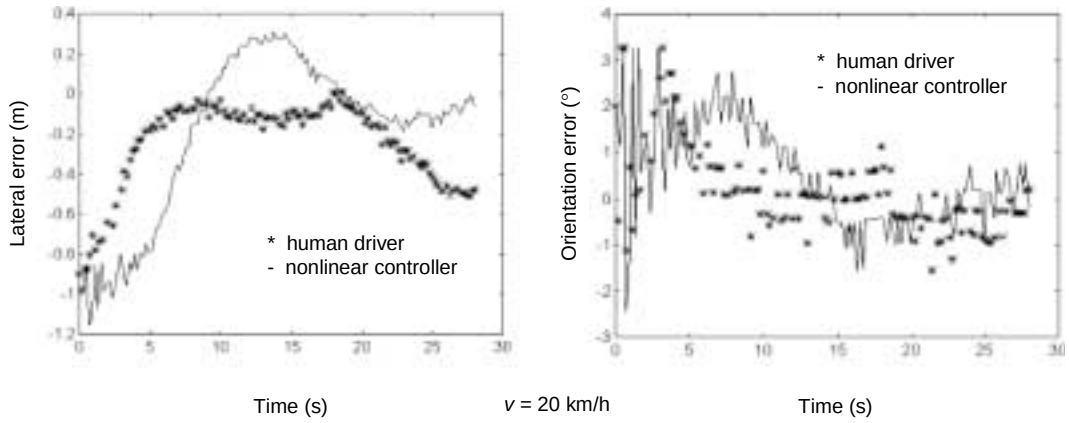

Fig. 9 Comparison between automatic guidance and human driving at $v = 20$ km/h

ing of car-like vehicles. In fact, it has been implemented on a real commercial vehicle slightly modified so as to allow for autonomous operation and tested on two different private circuits.

- A key advantage of the proposed method over other nonlinear control techniques relies on its ability to provide a priori design of the system transient response by proper fitting of constants K_d and K_p, while providing stable steady state response.
- Vehicle commanded actuation is taken into account by considering the current velocity in the design of the controller coefficients. This permits to adapt the steering angle as a function of driving conditions at not high energy expense from the control signal point of view.
- As demonstrated in practical trials, driving precision achieved by the lateral control law is as accurate as that of a human driver under normal conditions.

Nonetheless, in spite of having achieved some promising results there is still much space for improvement concerning vehicle stability and oscillations. Indeed, our current work focuses on accounting for more precise vehicle models including actuator dynamics and nonlinearities. Accordingly, a new nonlinear control law should be developed in an attempt to increase stability and comfortability when driving at high speed.

Acknowledgments

This work has been funded by the *Comisión Interministerial de Ciencia y Tecnología (CICYT)* through research project DPI2002-04064-C05-04, as well as by the generous support of the Industrial Automation Institute of the CSIC (*Consejo Superior de Investigaciones Cientificas*).

References

[1] J. Ackermann and W. Sienel, "Robust control for automated steering," in *Proc. of the 1990 American Control Conference, ACC90*, San Diego, CA, 1990, pp. 795–800.

[2] A. Broggi, M. Bertozzi, A. Fascioli, and G. Conte, *Automatic Vehicle Guidance: the Experience of the ARGO Autonomous Vehicle*. Singapore: World Scientific, 1999.

[3] R. H. Byrne, C. T. Abdallah, and P. Dorato, "Experimental results in robust lateral control of highway vehicles," *IEEE Control Systems Magazine*, vol. 18, no. 2, pp. 70–76, 1998.

[4] S. Cameron and P. Proberdt, *Advanced Guided Vehicles: Aspects of the Oxford AGV Project*. Singapore: World Scientific, 1994.

[5] L. Cordesses, P. Martinet, B. Thuilot, and M. Berducat, "GPS-based control of a land vehicle," in *Proc. of IAARC/IFAC/IEEE International Symposium on Automation and Robotics in Construction ISARC'99*, Madrid, Spain, September 1999.

[6] T. Hessburg and M. Tomizuka, "Fuzzy logic control for lateral vehicle guidance," *IEEE Control System Magazine* vol. 14, pp. 55-63, August 1994.

[7] J. Kosecka, R. Blasi, C. J. Taylor, and J. Malik, "Vision-based lateral control of vehicles," in *Proc. of Intelligent Transportation Systems Conference*, Boston, 1997.

[8] J. Luo and P. Tsiotras, "Control design for systems in chained form with bounded inputs," in *Proc. of American Control Conference*, Philadelphia, PA. June 1998.

[9] M. A. Sotelo, F. J. Rodriguez, L. Magdalena, L. M. Bergasa, and L. Boquete, "A color vision-based lane tracking system for autonomous driving on unmarked roads," *Autonomous Robots*, vol. 16, pp. 95–116, January 2004.

[10] H. Sussmann, E. Sontag, and Y. Yang, "A general result on the stabilization of linear systems using bounded controls," *IEEE Trans. on Automatic Control*, vol. 39, no. 12, pp. 2411–2425, January 1994.

[11] C. J. Taylor, J. Kosecka, R. Blasi, and J. Malik, "A comparative study of vision-based lateral control strategies for autonomous highway driving," *The International Journal of Robotic Research*, vol. 18, no. 5, pp. 442–453, 1999.

Biography

Miguel Ángel Sotelo received the Dr. Ing. degree in Electrical Engineering in 1996 from the Technical University of Madrid, and the Ph.D. degree in Electrical Engineering in 2001 from the University of Alcalá, Alcalá de Henares, Madrid, Spain. From 1993 to 1994 he has been a Researcher at the Department of Electronics, University of Alcala, where he is currently an Associate Professor. His research interests include Real-time Computer Vision, Control Applications, and Intelligent Transportation Systems for autonomous and assisted vehicles. He has been recipient of the Best Research Award in the domain of Automotive and Vehicle Applications in Spain, in 2002. He is the author of more than 50 refereed publications in international journals, book chapters, and conference proceedings. He is an active reviewer of several journals or transactions concerning Robotics, Control, and Intelligent Transportation Systems. Professor Sotelo is member of IEEE.

